Phase diagram of the selenide kesterite photovoltaic materials and NMR investigation of Cu/Zn disorder in CZTSe

Léo Choubrac, Alain Lafond, Michaël Paris, Catherine Guillot-Deudon and Stephane Jobic

Electronic Supporting Information

Experimental

Synthesis
The compounds were prepared by the solid state reaction of Cu, Zn, Sn, and S powders in the appropriate ratios in evacuated, sealed, fused silica tubes. They were heated at 750 °C (ramp 300 °C/h) for 170 h and then cooled down at 20 °C/h. The obtained powders were then ground and pressed into pellets which were again put into a sealed tube. The second heating sequence was: ramp 300 °C/h; plateau 750 °C; cooling ramp 50 °C/h. For some samples, attention was paid to the cooling mode at the end of the heating process. Samples were heated at 350 °C for 2 days and subsequently ice-quenched (sample $A2_Q$). A part of the obtained samples was reheated at 350 °C for 2 days, slow cooled down to 150°C (2 °C/h), annealed at this temperature for 1 day and finally slow cooled to room temperature. For example, from sample A2 (see Table 1) we got sample $A2_Q$ (quenched) and sample $A2_S$ (slow cooled).

X-ray diffraction
The powder X-ray diffraction patterns of the studied samples were measured on a D8-Bruker advance diffractometer (λ = 1.540596 Å), equipped with a LynxEye detector, in the 8-100 ° 2θ range with a 0.011 ° 2θ-step and a record time of 0.4 s/step. The analysis of the obtained patterns was performed with the use of the Jana2006 program[1].

For the single crystal analysis, a complete data set of Bragg reflections was collected on a Bruker-nonius Kappa CCD diffractometer with a crystal to detector distance of 25 mm and an exposure time of 10 s per frame. Lattice parameters and integrated intensities of the Bragg reflections were extracted from the measured images with the help of the Nonius program package[2]. The absorption correction and the crystal structure refinement were done with JANA2006. Experimental details are given in Table SI1.

Electron-Probe Micro Analyses
These analyses were performed on polished sections of the products imbedded in epoxy. The polishing process is known to not affect the surface composition of this kind of samples.

The operating conditions were: accelerating voltage 20 kV, current 20 nA. The standards were (element, emission line, counting time for one spot analysis): Cu metal (Cu Kα, 10 s), ZnS (Zn Kα, 10 s), SnO_2 (Sn Lα, 20 s), FeS_2 (S Kα, 20 s).

NMR spectroscopy
The ^{65}Cu and ^{119}Sn NMR spectra were acquired on a Bruker Avance III 300 MHz spectrometer with a 4 mm CP-MAS probe. In all cases, a full shifted echo acquisition sequence ($\theta - \tau - 2\theta - acq$) was used to obtain an absorption mode only line shape. For ^{119}Sn spectra, θ was set to $\pi/2$ for a radiofrequency (RF) field of 80 kHz and τ to 1.9 ms (slow cooling) or 1.0 ms (ice-quench). For ^{65}Cu spectra, θ was $\pi/10$ for a RF field of 35 kHz and the τ values were 1.2 ms and 0.5 ms for the slow-cooled and ice-quenched samples, respectively. ^{119}Sn spectra were acquired under MAS (14 kHz) condition with a recycle time of 120 s whereas ^{65}Cu spectra were obtained under static condition and a recycle time of 1s. ^{119}Sn spectra were referenced to Me_4Sn using Ph_4Sn as a secondary reference (-121.15 ppm) and ^{65}Cu spectra were referenced at 0 ppm against solid state CuCl. The spectral decomposition was performed using the "dmfit" freeware package[3].

The chemical shift interaction is described by $\delta_{iso}=(\delta_{XX}+\delta_{YY}+\delta_{ZZ})/3$, the isotropic chemical shift, $\delta_{aniso}=\delta_{ZZ}-\delta_{iso}$ the chemical shift anisotropy and $\eta_{\delta}=(\delta_{YY}-\delta_{XX})/\delta_{aniso}$ the asymmetry with the $|\delta_{ZZ}-\delta_{iso}|\geq |\delta_{XX}-\delta_{iso}|\geq|\delta_{YY}-\delta_{iso}|$ convention against the tensor eigenvalues. Similarly, considering that the Electric Field Gradient (EFG) tensor eigenvalues fulfilled the $|V_{ZZ}|\geq|V_{XX}|\geq|V_{YY}|$ convention, the quadrupolar interaction is described by $C_Q=e.Q.V_{ZZ}/h$ (the quadrupolar coupling) and by $\eta_Q=(V_{YY}-V_{XX})/V_{ZZ}$ (the asymmetry). In the C_Q expression, e is the electron charge, h the Planck's constant and Q the quadrupole moment. When both the chemical shift and quadrupolar interactions must be taken into account together (as for ^{65}Cu there), the Euler's angles α, β and γ define the orientation of the chemical shift tensor principal axis system in the EFG one.

For the spectral decomposition shown in Figure 1, α and γ are undetermined since both chemical shift and EFG tensors are axial. Error is estimated to 15 ppm on δ_{iso} and δ_{aniso} , 0.1 MHz on C_Q and 0.1 on the asymmetry parameters, η_{δ} and η_Q. Error on β is 5 ° and 10 ° for line W and N, respectively.

Raman spectroscopy

Raman spectra recorded at 514.5 nm excitation wavelength, were acquired in back scattering configuration on a Jobin-Yvon T64000 spectrometer coupled to a microscope (spot surface ~ 5 μm^2). As the laser excitation could induce modifications of the spectra (thermal effects and/or ordered to disordered phase transition within the kesterite structure), all measurements were performed with low power density of the incident laser close to 0.02 mW/μm^2.

Results

Powder X-ray diffraction

In the case of $A2_S$ and $A2_Q$ samples the full pattern matching refinements lead to very close unit cell parameters ($V(A2_S)$ = 367.51(2) $Å^3$ and $V(A2_Q)$ = 367.55(4) $Å^3$) but the c/a ratio are significantly different: 1.99119(8) and 1.9938(2) for the slow cooled and quenched samples respectively.

Single crystal investigation

Stannite (ST) and kesterite (KS) structures belong to different point group, namely -42m and -4. Then, Bragg reflections are not averaged in the same way in I-4m2 and I-4 space groups leading to a large difference in the numbers of unique reflections in both space groups. It is then very difficult to directly compare the residual factors obtained in refining the stannite and kesterite structural models. On the other hand, there is evidence that, as in the case of the pure sulfide CZTS compound, Cu/Zn disorder can occur within the cationic plane located at z=0.25 of the kesterite structure. If Cu and Zn atoms are randomly distributed within this layer then the whole structure becomes more symmetric and the so-called disordered kesterite (dis-KS) has to be described in the I-4m2 space group. It is then possible to compare the quality of the refinements using the ST and the dis-KS structures. Table SI2 gives the main results of the structure refinements of $Cu_2ZnSnSe_4$ in ST and the dis-KS structures. As previously mentioned, these two structures are close but the lowest residual factors for the disordered-kesterite structure and the homogeneity of the atomic displacement factors indicate that the structure of $Cu_2ZnSnSe_4$ is likely not stannite. In addition, the cation-anion bond distances are very close to those expected: Cu(2a)-Se = 2.4312(8) Å, Cu/Zn(4d)-Se = 2.4392(7) Å and Sn(2b)-Se = 2.5453(7) Å.

This result is in agreement with that Nateprov et al.,[4] but is more accurately described here. On one hand the previous structural investigations were performed on 2 samples whose compositions were determined by EDX measurements. One of the given compositions indicates a large excess of cations while refinement was done considering a stoichiometric sample. This structure cannot accommodate more than 4 cations taking into account the charge balance. On the other hand some inconsistencies in the comparison of the residual parameters are noted, for crystal I, the R value are 2.63% and 2.91 % for ST and dis-KS respectively while the corresponding wR values are 6.59% and 5.56%. Thus it is hard to conclude which is the best refinement. Our measured residual factors R(obs)/wR(obs) are less ambiguous (3.06/10.97 and 2.75/9.94 for stannite and kesterite respectively).

References
1. V. Petříček, M. Dušek and L. Palatinus, *Z. Für Krist. - Cryst. Mater.*, 2014, **229**, 345–352.
2. *Nonius, Kappa CCD Program Package*, Nonius B.V., Delft, The Netherlands, 1999.
3. D. Massiot, F. Fayon, M. Capron, I. King, S. Le Calvé, B. Alonso, J.-O. Durand, B. Bujoli, Z. Gan and G. Hoatson, *Magn. Reson. Chem.*, 2002, **40**, 70–76.
4. A. Nateprov, V. C. Kravtsov, G. Gurieva and S. Schorr, *Surf. Eng. Appl. Electrochem.*, 2013, **49**, 423–426.

Tables

<div align="center">Table SI1: Single crystal data collection details</div>

Crystal data	
Chemical formula	Cu_2Se_4SnZn
M_r	627.02
Crystal system, space group	Tetragonal, $I-42m$
Temperature (K)	293
a, c (Å)	5.69647(5), 11.3394 (2)
V (Å^3)	367.965(6)
Z	2
$F(000)$	548
D_x (Mg m^{-3})	5.658
Radiation type	Mo $K\alpha$
θ range (°) for cell measurement	6.48–34.91
μ (mm^{-1})	31.95
Crystal shape	Block (pyramid)
Colour	Black
Crystal size (mm)	$0.03 \times 0.03 \times 0.015$
Data collection	
Diffractometer	Nonius CCD diffractometer
Monochromator	Graphite
Scan method	phi,ω scans
Absorption correction	Gaussian - Jana2006
T_{min}, T_{max}	0.1892, 0.3767
No. of measured, independent and observed [$I > 2\sigma(I)$] reflections	3282, 447, 411
R_{int}	0.056
$(\sin \theta/\lambda)_{max}$ (Å^{-1})	0.807
Range of h, k, l	$h = -9{\rightarrow}9, k = -7{\rightarrow}9, l = -13{\rightarrow}18$
Refinement	
Refinement on	F^2
$R[F^2 > 2\sigma(F^2)], wR(F^2), S$	0.027, 0.099, 1.77
No. of reflections	411
No. of parameters	14
Weighting scheme	$w = 1/(\sigma^2(I) + 0.001936I^2)$
$\Delta\rho_{max}, \Delta\rho_{min}$ (e.Å^{-3})	1.31, -1.24

Table SI2: Comparison of results for the single crystal structure investigation of $Cu_2ZnSnSe_4$ in ST and dis-KS structural models.

Structural model	stannite	disordered kesterite
2a	Zn	Cu
4d	Cu	Cu/Zn (50/50)
Ueq(2a)	0.0211(4)	0.0182(3)
Ueq(4d)	0.0127(3)	0.0141(3)
R/wR(obs)	3.06/10.97	2.75/9.94
Fourier-difference map (e-/Å^3)	0.93/-0.69	1.31/-1.24
# hkl I/σ(I)>2.0	411	411
# refined parameters	14	14

Table SI3: Average compositions of the studied compounds and the corresponding coordinates in the Cu$_2$Se/ZnSe/SnSe$_2$ ternary diagram

Label	Average composition	Cu$_2$S at%	ZnS at%	SnS$_2$ at%
S1	Cu$_{1.999}$Zn$_{1.010}$Sn$_{0.995}$Se$_4$	33.3	33.6	33.1
S2	Cu$_{1.936}$Zn$_{0.964}$Sn$_{1.039}$Se$_4$	32.6	32.4	35.0
S3	Cu$_{1.911}$Zn$_{1.011}$Sn$_{1.036}$Se$_4$	31.8	33.7	34.5
A1	Cu$_{1.828}$Zn$_{1.128}$Sn$_{0.978}$Se$_4$	30.3	37.4	32.4
A2	Cu$_{1.751}$Zn$_{1.196}$Sn$_{0.957}$Se$_4$	28.9	39.5	31.6
A3	Cu$_{1.640}$Zn$_{1.290}$Sn$_{0.945}$Se$_4$	26.8	42.2	30.9
A4	Cu$_{1.693}$Zn$_{1.239}$Sn$_{0.951}$Se$_4$	27.9	40.8	31.3
B1	Cu$_{1.925}$Zn$_{1.061}$Sn$_{0.966}$Se$_4$	32.2	35.5	32.3
AB1-1	Cu$_{1.984}$Zn$_{1.065}$Sn$_{0.987}$Se$_4$	32.6	35.0	32.4
AB1-2	Cu$_{1.936}$Zn$_{1.147}$Sn$_{0.972}$Se$_4$	31.4	37.2	31.5
AE1	Cu$_{1.765}$Zn$_{1.105}$Sn$_{0.987}$Se$_4$	29.7	37.1	33.2
AE2	Cu$_{1.589}$Zn$_{1.168}$Sn$_{1.009}$Se$_4$	26.7	39.3	34.0

Figures
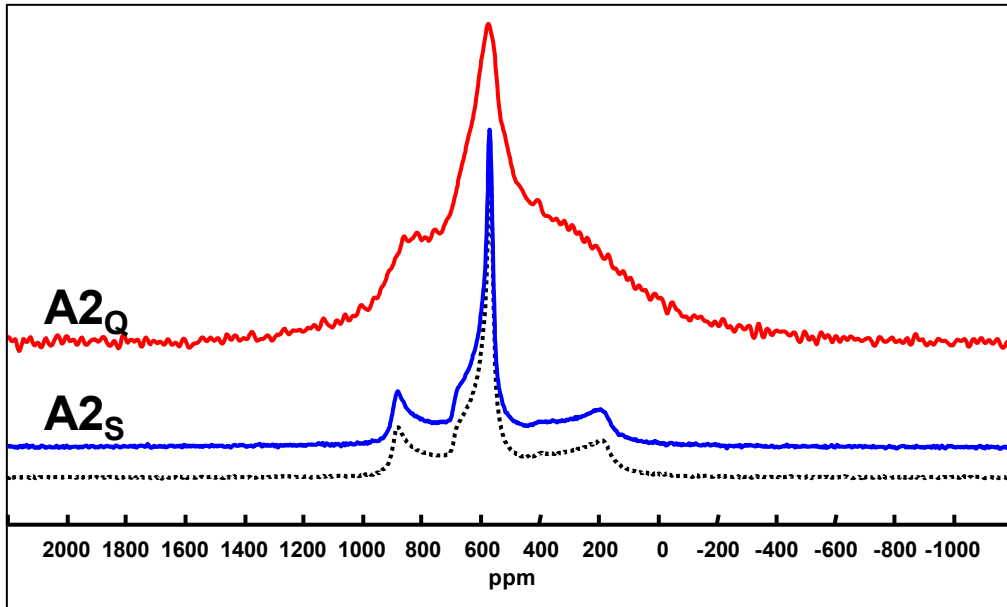
Figure SI1: ^{65}Cu static NMR spectra for A2$_S$ (slow cooled) and A2$_Q$ (quenched) samples. The spectrum for the slow cooled sample (non stoichiometric) is very close to that of the stoichiometric Cu$_2$ZnSnSe$_4$ compound (in dot line).
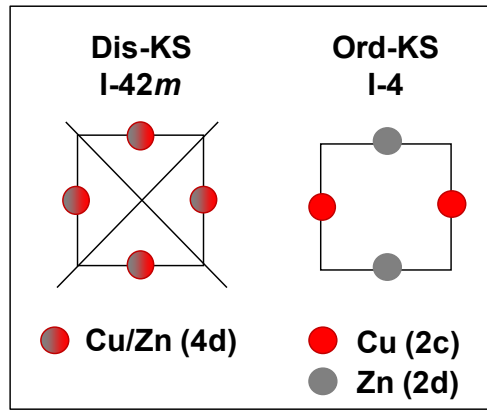
Figure SI2: Representation of the cationic (Cu and Zn) distribution in the z = 1/4 plane for the disordered kesterite (*I*-42*m* space group) and the ordered kesterite (*I*-4 space group).
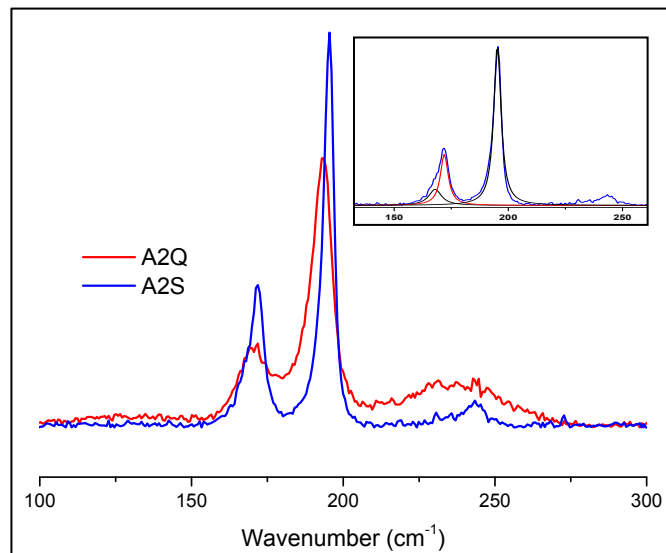
Figure SI3: Raman spectra of slightly non-stoichiometric quenched (A2$_Q$) and slow cooled samples (A2$_S$) with formula of $Cu_{1.171}Zn_{1.196}Sn_{0.957}Se_4$. The inset gives the spectral decomposition for A2$_S$.
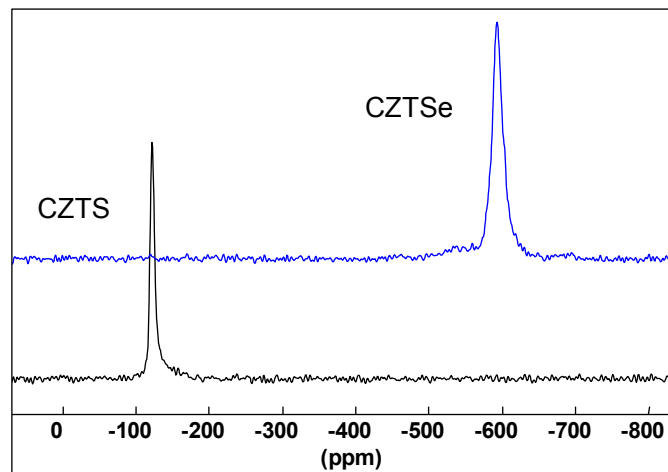
Figure SI4: Comparison of ^{119}Sn MAS spectra for pure sulphide CZTS and pure selenide CTZSe. The overall shift is of -470 ppm for CZTSe with respect to CZTS.